EXHIBIT B

THE JOURNAL OF BIOLOGICAL CHEMISTRY
Vol. 278, No. 25, Issue of June 20, pp. 22331–22340, 2003
Printed in U.S.A.

Catalytic Properties of ADAM19*

Received for publication, March 18, 2003
Published, JBC Papers in Press, April 7, 2003, DOI 10.1074/jbc.M302781200

Valérie Chesneau‡, J. David Becherer§, Yufang Zheng‡¶, Hediye Erdjument-Bromage‖, Paul Tempst‖, and Carl P. Blobel‡**

From the ‡Cellular Biochemistry and Biophysics Program, ‖Molecular Biology Program, Sloan-Kettering Institute, Memorial Sloan-Kettering Cancer Center, New York, New York 10021, the §Department of Biochemical and Analytical Pharmacology, GlaxoSmithKline, Research Triangle Park, North Carolina 27709, and ¶Graduate Program in Physiology, Biophysics, and Molecular Medicine, Weill Graduate School of Medical Science of Cornell University, New York, New York 10021

ADAMs are membrane-anchored glycoproteins with functions in fertilization, heart development, neurogenesis, and protein ectodomain shedding. Here we report an evaluation of the catalytic activity of recombinantly expressed soluble forms of ADAM19, a protein that is essential for cardiovascular morphogenesis. Proteolytic activity of soluble forms of ADAM19 was first demonstrated by their autocatalytic removal of a purification tag (Myc-His) and their ability to cleave myelin basic protein and the insulin B chain. The metalloprotease activity of ADAM19 is sensitive to the hydroxamic acid-type metalloprotease inhibitor BB94 (batimastat) but not to tissue inhibitors of metalloproteases (TIMPs) 1–3. Moreover, ADAM19 cleaves peptides corresponding to the known cleavage sites of tumor necrosis factor-α (TNF−α), TNF-related activation-induced cytokine (TRANCE, also referred to as osteoprotegerin ligand), and kit ligand-1 (KL-1) *in vitro*. Although ADAM19 is not required for shedding of TNFα and TRANCE in mouse embryonic fibroblasts, its overexpression in COS-7 cells results in strongly increased TRANCE shedding. This suggests a potential role for ADAM19 in shedding TRANCE in cells where both molecules are highly expressed, such as in osteoblasts. Interestingly, our results also indicate that ADAM19 can function as a negative regulator of KL-1 shedding in both COS-7 cells and mouse embryonic fibroblasts, instead of acting directly on KL-1. The identification of potential *in vitro* substrates offers the basis for further functional studies of ADAM19 in cells and in mice.

ADAMs[1] are a family of type I transmembrane glycoproteins that contain a disintegrin and metalloprotease (for recent reviews see Refs. 1–3). Since the discovery of the first recognized ADAM, the heterodimeric sperm protein fertilin (4–6), the ADAM family has been growing rapidly to reach a total of 33 members identified in a variety of species, including mammals, *Xenopus laevis*, *Drosophila melanogaster*, and *Caenorhabditis elegans*. There are now 26 recognized ADAM homologues in the mouse (for details, see www.gene.ucl.ac.uk/nomenclature/genefamily/metallo.html and www.people.virginia.edu/~jw7g/Table_of_the_ADAMs.html). Although all ADAMs share a common domain organization, consisting of a pro-, metalloprotease, disintegrin, cysteine-rich, epidermal growth factor-like, transmembrane, and a cytoplasmic domain (see Fig. 1), only 16 of the 26 mouse members present a fully conserved metzincin consensus catalytic site (HE*X*GH*XX*G*XX*HD (7–10)) and can thus be expected to be active metalloproteases.

Numerous membrane-anchored proteins, including cytokines, growth factors, receptors, adhesion molecules, and enzymes, have been shown to undergo proteolytic release from the plasma membrane (11, 12). This event, which is thought to regulate the function of the substrate proteins, is called protein ectodomain shedding. Inhibitor studies have revealed that most shedding events are mediated by metalloproteases (13). ADAMs have been clearly implicated in the shedding of several proteins, although some matrix metalloproteinases (MMP) may also act as sheddases in specific circumstances (14–16). For example, studies of mice lacking functional TACE (TNFα-converting enzyme, ADAM17 (17, 18)) indicate that this protease is the major inducible TNFα sheddase *in vivo* (18). Additionally, analyses of cells derived from TACE-deficient animals suggest that this ADAM is also responsible for the processing of transforming growth factor-α, L-selectin, and p75 TNF receptor (19), as well as interleukin-1 receptor II (20) and HER4, a member of the epidermal growth factor receptor family (21). Functional Kuzbanian, the putative ADAM10 orthologue in *D. melanogaster*, is required for proper Notch signaling and is thought to trigger the second cleavage of this transmembrane receptor protein (22–24). TACE, ADAM10, and ADAM9 have also been proposed as candidates for the role of amyloid precursor protein α-secretase (25–28), although hippocampal neurons cultured from *adam9−/−* mice seem to process amyloid precursor protein as well as those derived from wild type animals (29). However, little is currently known about the catalytic activity of other ADAMs. Furthermore, the enzymes responsible for the processing of many proteins that are shed

* This work was supported by a grant from GlaxoSmithKline (to C. P. B.), by the Memorial Sloan-Kettering Cancer Center Support Grant NCI-P30-CA-08748, by the Samuel and May Rudin Foundation, and by the DeWitt Wallace Fund. The costs of publication of this article were defrayed in part by the payment of page charges. This article must therefore be hereby marked "*advertisement*" in accordance with 18 U.S.C. Section 1734 solely to indicate this fact.

** To whom correspondence should be addressed: Cellular Biochemistry and Biophysics Program, Sloan-Kettering Institute, Memorial Sloan-Kettering Cancer Center, Box 368, 1275 York Ave., New York, NY 10021. Tel.: 212-639-2915; Fax: 212-717-3047; E-mail: c-blobel@ski.mskcc.org.

[1] The abbreviations used are: ADAM, a disintegrin and a metalloprotease; AP, alkaline phosphatase; EC, extracellular domain; FBS, fetal bovine serum; KL, kit ligand; MBP, myelin basic protein; mEFs, mouse embryonic fibroblasts; MMP, matrix metalloproteinase; PV, pervanadate; TGN, trans-Golgi network; TIMP, tissue inhibitor of metalloproteases; TNFα, tumor necrosis factor α; TRANCE, TNF-related activation induced cytokine; MALDI-reTOF MS, matrix-assisted laser desorption ionization reflectron time-of-flight mass spectrometry; CHO, Chinese hamster ovary; PMA, phorbol 12-myristate 13-acetate; Bistris, 2-[bis(2-hydroxyethyl)amino]-2-(hydroxymethyl)propane-1,3-diol; NBT/BCIP, nitro blue tetrazolium chloride/5-bromo-4-chloro-3-indoyl phosphate.

from the plasma membrane remain to be identified.

ADAM19, also know as meltrin β (30), is a widely expressed protein, but its mRNA is particularly abundant in bone, heart, and lung (31). Mouse ADAM19 cDNA has been isolated from a C2C12 muscle cell library, and the encoded protein presents the classical domain organization of the members of the ADAM family, as well as an intact consensus catalytic site (HEIGHNFGMSHD; Fig. 1). Its closest homologues are ADAM12 (meltrin α (30)), ADAM13 (32), and ADAM33 (33–35). Human ADAM19 cDNA has also been isolated recently (36), and a soluble form of the protein has been recombinantly expressed in 293T cells (37). This initial attempt to characterize the catalytic activity of ADAM19 focused on the cleavage of α_2-macroglobulin, a suicide inhibitor that covalently binds to the protease and inactivates it after cleavage. Overexpression experiments in L929 cells also recently suggested that ADAM19 may participate in the shedding of neuregulin, a member of the epidermal growth factor family, and more specifically of its β isoforms (38). Finally, interest in the characterization of ADAM19 catalytic activity is further stimulated by the recent discovery that this protein is essential for cardiovascular morphogenesis in mice.[2]

As a first step in the biochemical characterization of ADAM19, we expressed and purified two soluble recombinant forms of the mouse enzyme. These proteins are active metalloproteases and were used to identify several *in vitro* substrates among short peptides corresponding to the region surrounding the cleavage site of shed proteins. We also present the analysis of ADAM19 sensitivity toward tissue inhibitors of metalloproteinases (TIMPs) and the hydroxamic inhibitor BB94 *in vitro*, and we discuss the implications of our findings for the understanding of the function of this metalloprotease. Finally, using cell-based assays, we assessed the potential physiological relevance of ADAM19 in shedding candidate substrates (TNF-α, TRANCE, and KL-1).

MATERIALS AND METHODS

Reagents—Mutagenesis oligonucleotides were obtained from GeneLink. The pFastBac1 vector, competent DH10Bac cells, Sf9 cells, serum-free medium-adapted Hi5 cells, and serum-free insect cell media (Sf-900 II SFM and Ultimate Insect serum-free medium) were purchased from Invitrogen. TIMP-1 and -2 were kindly provided by Dr. Gillian Murphy (University of East Anglia, UK), and the His-tagged recombinant N-terminal domain of TIMP-3 was a gift from Dr. Hideaki Nagase (Kennedy Institute, UK). The kit ligand 1 (KL-1) cDNA was provided by Dr. Peter Besmer (Memorial Sloan-Kettering Cancer Center, New York).

Construction of the ADAM19(EC) and ADAM19(MP) Expression Plasmids—All nucleotide numbers refer to mouse ADAM 19 cDNA sequence (GenBank™ accession number AF019887 (31)). pcDNA3-EK-Fc was originally generated by inserting a sequence encoding an enterokinase cleavage site (EK; amino acid sequence DDDDK) at the *Bam*HI site of the pcDNA3-Fc vector (39). pFasBac1-EK-Fc was created by transferring the sequence encoding the enterokinase site followed by the human IgG-Fc domain of pcDNA3-EK-Fc between the *Bam*HI and *Xba*I sites of pFasBac1. pcDNA3/ADAM19(EC)EK-Fc and pFastBac1/ADAM19(EC)EK-Fc were made to express a soluble ADAM19 extracellular domain (EC) fused to the Fc portion of the human IgG in mammalian and insect cells, respectively. Specifically, PCR was used to generate a fragment corresponding to bases 11–2175 of mouse ADAM19 cDNA, bearing *Bcl*I sites on both 5′ and 3′ ends. In a two step-PCR procedure, the same fragment carrying the adenine 1075 to cytosine and guanine 1076 to adenine mutations was created. These mutations lead to the production of inactive protease carrying a glutamate to alanine mutation in the catalytic site (E/A mutant). After digestion with *Bcl*I, the two restriction products were subcloned at the *Bam*HI site of pcDNA3-EK-Fc and pFastBac1-EK-Fc.

In a second step, we generated plasmids to express soluble C-terminally Myc- and poly-His-tagged wild type and E/A mutant ADAM 19 extracellular domains. The *Sal*I-*Xba*I restriction fragments of pFastBac1/ADAM19(EC)EK-Fc and pFastBac1/ADAM19($EC_{E/A}$)EK-Fc were replaced by the corresponding digestion product of pBlSK$^+$-MycHis. The latter plasmid carries the sequence encoding a Myc tag followed by a hexa-histidine tag (amino acid sequence: EQKLISEEDLHHHHHH) subcloned inbetween the *Bam*HI and *Xba*I restriction sites of pBluescript SK(+) (Stratagene). The resulting constructs were used to express the recombinant proteins in insect cells. Finally, pcDNA3/ADAM19(EC)-MycHis and pcDNA3/ADAM19($EC_{E/A}$)-MycHis were obtained by replacing the *Xcm*I-*Xba*I restriction fragment of pcDNA3/ADAM19(EC)EK-Fc by those of pFastBac1/ADAM19(EC)-MycHis or pFastBac1/ADAM19($EC_{E/A}$)-MycHis to allow the expression of the same proteins in mammalian cells.

Constructs to express a soluble ADAM19 containing only the pro- and metalloprotease domains (MP constructs) were generated in two steps. A fragment corresponding to nucleotides 8–1312 of ADAM19 cDNA and carrying a *Bam*HI site on both ends was generated by PCR. Both the wild type and mutated (adenine 1075 to cytosine and guanine 1076 to adenine mutations encoding the inactive mutant) ADAM19 sequences were amplified. These fragments were introduced at the *Bam*HI site of pBlSK$^+$-MycHis (see above), and the *Eco*RI-*Xba*I fragments of the resulting constructs were subcloned into the corresponding restriction sites of pcDNA3 and pFastBac1. All constructs were sequenced to rule out undesired mutations.

Production of the Anti-ADAM19($EC_{E/A}$)EK-Fc Polyclonal Antibodies—pcDNA3/ADAM19($EC_{E/A}$)EK-Fc was used to establish CHO lines stably expressing and secreting the extracellular domain of the catalytically inactive $ADAM19_{E/A}$ fused to the Fc domain of the human IgG. After transfection using LipofectAMINE (Invitrogen), positive clones of CHO cells were selected in F-12 medium containing 5% fetal bovine serum (FBS), 1 unit/ml penicillin, 1 μg/ml streptomycin, and 500 μg/ml of the antibiotic G418 (geneticin; Invitrogen). Expression was monitored by Western blot analysis using a rabbit anti-human IgG, Fcγ-specific antibody (Pierce). To produce recombinant ADAM19, stably transfected cells were grown for 3 days in serum-free Opti-MEM-I (Invitrogen). Conditioned media were collected, and the cell debris were removed by filtration through a 0.22-μm filter. The soluble ADAM19($EC_{E/A}$)EK-Fc fusion protein was purified by affinity chromatography using a 1-ml Hi-Trap rProtein A column (Amersham Biosciences), as described previously (40). Polyclonal antibodies against the recombinant protein were raised in New Zealand White rabbits by Covance.

Expression of Recombinant ADAM19 Proteins in Mammalian Cells—COS-7 cells were grown in Dulbecco's modified Eagle's medium supplemented with 5% FBS, 1 unit/ml penicillin, and 1 μg/ml streptomycin. One day prior to transfection, cells were plated at the density of 1.5×10^5 per well of 6-well plates. Cells were transiently transfected with 2 μg of pcDNA3/ADAM19(EC)-MycHis and pcDNA3/ADAM19($EC_{E/A}$)-MycHis using LipofectAMINE. The expression step was carried out in Opti-MEM-I. After 48 h, culture media were collected and incubated with 20 μl of Talon™ resin (Clontech) pre-equilibrated in 50 mM sodium phosphate, pH 7.0, 300 mM NaCl. The MycHis-tagged proteins bound to the resin were analyzed by Western blot using the monoclonal anti-Myc antibody 9E10 at the 1:1000 final dilution.

Expression of Recombinant ADAM19 Proteins in Insect Cells—Recombinant baculoviruses were obtained using the Bac-to-Bac expression system as recommended by the manufacturer (Invitrogen). Briefly, recombinant bacmids were obtained by transforming DH10Bac competent cells with 1 μg of pFastBac1/ADAM19(EC)-MycHis, pFastBac1/ADAM19($EC_{E/A}$)-MycHis, pFastBac1/ADAM19(MP)-MycHis, or pFastBac1/ADAM19($MP_{E/A}$)-MycHis. Transfecting Sf9 cells with the recombinant bacmids led to the production of a first viral stock of titer ~5×10^7 plaque-forming units/ml, which was subsequently amplified. This amplified viral stock was then used to infect Hi5 cells to express the recombinant ADAM19s. The expression step was performed in Ultimate Insect serum-free medium. After 72 h, conditioned media were collected and centrifuged for 2 h at 20,000 × *g* and 4 °C to pellet the virus particles. The supernatants were frozen in a dry ice/ethanol bath, kept at −80 °C, and later used in proteolytic assays or as a source for ADAM19 purification.

Purification of Recombinant ADAM19 Proteins—Supernatants from the 20,000 × *g* centrifugation (see under "Expression of Recombinant ADAM19 Proteins in Insect Cells") were incubated with a minimal amount (~20 μl) of Talon™ metal affinity resin pre-equilibrated in 50 mM sodium phosphate, pH 7.0, 300 mM NaCl. The binding step was carried out in batch either overnight at 4 °C, or for 30 min at room temperature. After pelleting the resin, the unbound protein solution was removed, and the beads were packed into a small column. The resin was washed with a 20-fold volume of equilibration buffer, and the

[2] H. M. Zhou and C. P. Blobel, submitted for publication.

Myc-His-tagged proteins were eluted with 10 volumes of 50 mM sodium acetate, pH 5.0, 300 mM NaCl. The amount of protein in each fraction was estimated by SDS-PAGE followed by Gelcode Blue Reagent (Pierce) staining. The most concentrated fractions were combined and used immediately in proteolytic assays.

Proteolytic Assays—Self-proteolysis of recombinant ADAM19(EC)-MycHis was assayed in conditioned media by incubating 10 μl of the supernatant devoid of virus particles (see under "Expression of Recombinant ADAM19 Proteins in Insect Cells") with 10 μl of 50 mM Tris-HCl, pH 7.4 or 8.5, 300 mM NaCl for 16 h at 37 °C. Incubations were performed in the presence or absence of different protease inhibitors, as indicated. The amount of proteolysis was estimated by Western blot analysis using the monoclonal anti-Myc antibody 9E10 at the 1:1000 final dilution. Similar incubations performed with an aliquot of the purified wild type enzyme or of the inactive mutant were analyzed by either Western blot or SDS-PAGE followed by Gelcode Blue staining.

Bovine myelin basic protein (MBP; Sigma) was purified by electroelution from 12.5% SDS-polyacrylamide gels (40). Degradation assays by ADAM19(EC)-MycHis were performed by incubating purified MBP with an aliquot of purified enzyme in 50 mM Tris-HCl, pH 8.5, 200 mM NaCl for 1–6 h at 37 °C. Protease inhibitors were added as indicated. MBP degradation by recombinant TACE was assayed in 50 mM Tris-HCl, pH 7.4, 2 mM $CaCl_2$. Reaction products were analyzed by SDS-PAGE on 10% Bistris NuPage acrylamide gels (Invitrogen). Proteins were revealed using the Gelcode Blue Stain reagent.

The ability of ADAM19 to cleave insulin B chain (Sigma) and dinitrophenyl-labeled synthetic peptides corresponding to the 12 amino acids surrounding the processing site of selected membrane proteins known to be shed (41) was assayed as follows. Potential substrates at the final concentration of 100 μM were incubated in 50 mM Tris-HCl, pH 8.5, 150 mM NaCl for 6 h at 37 °C with an aliquot of wild type purified enzyme in the presence or absence of 1 mM 1,10-phenanthroline or with an aliquot of inactive mutant. Reactions were stopped by the addition of trifluoroacetic acid, and the cleavage products were subjected to matrix-assisted laser desorption ionization reflectron time-of-flight mass spectrometry (MALDI-reTOF MS) using a Bruker Ultraflex TOF/TOF instrument (Bruker Daltonics Inc.); in isolated cases, the sequences of the peptides were confirmed by operating the instrument in "LIFT" (laser induced fragmentation) mode; the resulting tandem MS/MS spectrum was then inspected for the y", b", and a" ion series in order to confirm the sequence provided (42). The theoretical protonated monoisotopic masses were calculated using PEPTIDEMASS software (43) at us.expasy.org/tools/peptide-mass.html.

Protein N-terminal Sequencing—Purified recombinant ADAM19 or protein mixtures from MBP degradation assays by either ADAM19 or TACE were separated on NuPage 10% Bistris acrylamide gels, transferred to a polyvinylidene difluoride membrane, and stained with Coomassie R-250. After destaining with 50% methanol, 10% acetic acid, the bands of interest were excised, and the N-terminal amino acids were identified by automated Edman degradation using an Applied Biosystems 494 automated sequenator, as described previously (44).

Generation of TNF, TRANCE, and KL-1 Expression Plasmids—To facilitate the detection of both precursor and shed forms of TNFα, TRANCE, and KL-1, all three proteins were expressed as fusion proteins bearing an alkaline phosphatase (AP) module in their extracellular domain. The engineering of pAPtag5-TNFα was described previously (45). pFLAG-mTRANCE (46) was used as a template to amplify a sequence encoding the FLAG tag followed by the full-length mouse TRANCE. An *Nhe*I site was introduced 6 nucleotides upstream of the beginning of the coding sequence, and TRANCE stop codon and following nucleotides were mutated to create a *Hin*dIII site. The PCR product, digested by *Nhe*I and *Hin*dIII, was subcloned inbetween the corresponding sites of pAPtag5 vector (Genhunter Corp.). The sequence encoding the full-length KL-1 cDNA was subcloned in-frame between the *Xho*I and *Xba*I sites of pAPtag5. Briefly, nucleotides 273–275 (GenBank™ accession number U44725) of KL-1 cDNA were mutated to introduce an *Xho*I site, and nucleotides 1016–1018 around the stop codon were changed to create an *Xba*I restriction site. All final constructs were sequenced to rule out any unwanted mutations. The resulting fusion proteins are schematized in Fig. 7*A*.

Shedding Assays—COS-7 cells seeded in 6-well plates were cotransfected with either pAPtag5-TRANCE or pAPtag5-KL-1 plasmids together with the control vector $pcDNA_3$, full-length wild type mouse ADAM19 expression plasmid ($pcDNA_3$-ADAM19), mouse ADAM19 inactive mutant expression vector ($pcDNA_3$-$ADAM19_{E/A}$), or $pcDNA_{3.1}$-mTACE (45), as indicated. Transfections were performed in Opti-MEM-I for 5 h, and cells were left to recover overnight in Dulbecco's modified Eagle's medium supplemented with 5% FBS, 1 unit/ml penicillin, and 1 μg/ml streptomycin. Mouse embryonic fibroblasts (MEFs) were prepared from 13.5-day-old wild type or ADAM19-deficient mouse embryos,[2] as described previously (14, 29, 47), and cultured in Dulbecco's modified Eagle's medium supplemented with 10% FBS, 1 unit/ml penicillin, and 1 μg/ml streptomycin for one or two passages prior to transfection. Seeded in 6-well plates, MEFs were transiently transfected with either pAPtag5-TNFα, pAPtag5-TRANCE, or pAPtag5-KL-1 using LipofectAMINE 2000 (Invitrogen). After 5 h, cells were allowed to recover overnight in complete growth medium.

The day following transfection, COS-7 cells and MEFs were washed once in phosphate-buffered saline and incubated for 1 h in Opti-MEM-I and then for 1 h in Opti-MEM-I containing either 25 ng/ml phorbol 12-myristate 13-acetate (PMA) or 100 μM pervanadate (PV) as described previously (45). Supernatants were collected, and cells were lysed in phosphate-buffered saline containing 1% Triton X-100 and a mixture of protease inhibitors (2 μg/ml leupeptin, 10 μg/ml soybean trypsin inhibitor, 500 μM iodoacetamide, and 1 mM 1,10-phenanthroline). His-tagged shed forms of TNFα-AP and TRANCE-AP were concentrated from supernatants using Talon™ metal affinity resin. Proteins were eluted from the resin using 0.5 M imidazole and analyzed by 8% SDS-PAGE. The AP activity was visualized in-gel using nitro blue tetrazolium chloride and 5-bromo-4-chloro-3-indoyl phosphate (NBT/BCIP) as described (45). Shed AP-KL-1 present in culture supernatants was either quantified by spectrometry using the AP substrate 4-nitrophenyl phosphate (45) or concentrated using concanavalin A-Sepharose (Amersham Biosciences). Proteins were then eluted from the resin using 50 mM Tris-HCl, pH 7.4, 0.5 M α-methyl-D-mannoside, and analyzed by 8% SDS-PAGE. COS-7 cell lysates were assayed for their content in ADAM19 by 8% SDS-PAGE under non-reducing conditions followed by Western blot using the anti-$ADAM19(EC_{E/A})$EK-Fc polyclonal antibodies at a 1:1000 final dilution. Antigen-antibody complexes were revealed using ECL (Amersham Biosciences).

RESULTS

Although ADAMs physiologically exist as transmembrane proteins, several members of the family have been successfully expressed as soluble metalloproteases (17, 40, 41, 48–52). The presence of the prodomain generally appeared necessary for the proper folding of the recombinant proteins, but the number of ADAM protein domains used to express an active protease varied from case to case. We therefore engineered two sets of constructs to express molecules either corresponding to the entire extracellular domain of ADAM19 (ADAM19(EC)), or composed of the pro- and metalloprotease only (ADAM19(MP)) (Fig. 1*A*). Recombinant proteins were C-terminally Myc- and His-tagged to facilitate both detection and purification. Additionally, inactive mutants bearing a glutamate to alanine substitution in their catalytic site (HEIGH > HAIGH) were expressed as controls.

Wild type and mutant ADAM19(EC)-MycHis retrieved from the culture media of infected Hi5 cells and transiently transfected COS-7 cells is shown in Fig. 1*B*. Both forms were expressed at a slightly higher level in insect cells. For example, about three times more COS-7 than Hi5 cells were necessary to produce comparable amounts of wild type recombinant ADAM19 presented in Fig. 1*B*. Also, both cell types were able to process and remove the ADAM19 prodomain, but again, the ratio of mature *versus* pro-form was higher in insect cells than in mammalian cells. These two observations prompted us to use baculovirus as the most efficient expression system for recombinant ADAM19. The size discrepancy between the mature forms produced by the two cell lines (65 kDa in Hi5 *versus* 67 kDa in COS-7 cells for the wild type protein, and 63 kDa in Hi5 *versus* 65 kDa in COS-7 cells for the mutant form) is likely to reflect differences in glycosylation, as often observed between insect and mammalian cells. However, this did not seem to affect recombinant ADAM19 proteolytic activity (see below). In both expression systems, the wild type enzyme also migrated slightly slower than the corresponding mutant (67 *versus* 65 kDa for the mutant in Hi5 cells). Nevertheless, both wild type and mutant ADAM19(EC)-MycHis were secreted, and

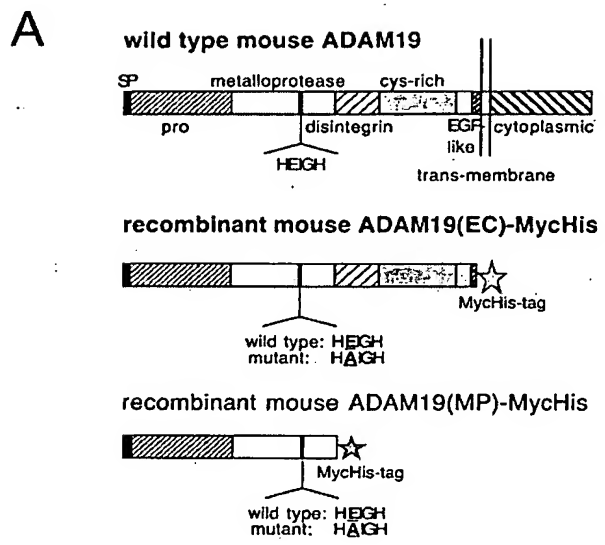

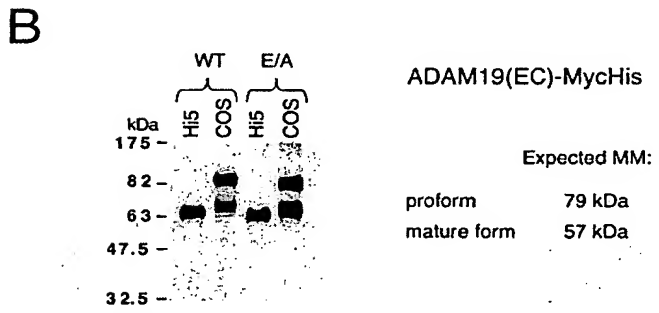

FIG. 1. *A*, schematic representation of the domain organization of mouse ADAM19 and recombinant ADAM19(EC)-MycHis and ADAM19(MP)-MycHis. *SP*, signal peptide; *pro*, metalloprotease domain; *cys-rich*, cysteine-rich domain; *EGF*, epidermal growth factor-like domain. *B*, expression of soluble ADAM19(EC)-MycHis in Hi5 and COS-7 cells. ADAM19(EC)-MycHis present in the conditioned medium from infected Hi5 cells or transiently transfected COS-7 cells was concentrated using metal-affinity Talon™ beads. Proteins were then separated by 8% SDS-PAGE, transferred to nitrocellulose, and detected by Western blotting using the anti-Myc antibody 9E10. Double the amount of material compared with the mutant had to be used to visualize wild type (*WT*) ADAM19(EC)-MycHis from COS-7 cells. The molecular masses of protein markers are indicated in kDa.

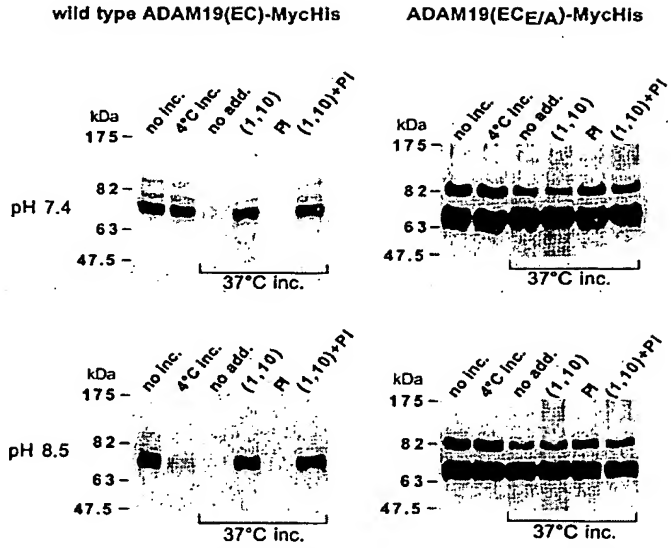

FIG. 2. **Evidence for autocatalytic processing of recombinant ADAM19.** 10 μl of conditioned medium from Hi5 cells expressing either the wild type ADAM19(EC)-MycHis (*left panels*) or its mutant inactive counterpart (*right panels*) were incubated with 10 μl of 50 mM Tris-HCl, 300 mM NaCl, at either pH 7.4 (*upper panels*) or pH 8.5 (*lower panels*). Lanes labeled *no inc.* (no incubation) correspond to control aliquots kept at −20 °C. Incubations were carried out for 16 h at either 4 or 37 °C. In the *4th* to *6th lanes*, inhibitors were added to the reaction mixtures: (*1,10*), 1,10-phenanthroline 1 mM final concentration; *PI*, inhibitor mixture containing leupeptin (2 μg/ml final concentration), soybean trypsin inhibitor (10 μg/ml), and iodoacetamide (500 μM); and (*1,10*)+*PI*, a combination of all above inhibitors. Recombinant ADAM19 integrity after incubation was assayed by 8% SDS-PAGE and Western blotting with the anti-Myc antibody, 9E10.

polyclonal antibodies raised against the extracellular domain of the catalytically inactive ADAM19$_{E/A}$ fused to the Fc domain of the human IgG recognized wild type ADAM19(EC)-MycHis as well as the corresponding mutant (data not shown), arguing that the point mutation does not affect folding of recombinant ADAM19.

We then investigated the stability of recombinant ADAM19(EC)-MycHis in conditioned medium from infected Hi5 cells at different pH values (Fig. 2). As shown by Western blot analysis with an anti-Myc antibody, the C-terminal tags of wild type recombinant ADAM19 are removed upon incubation at 37 °C and pH 7.4 (Fig. 2, *upper panel*). This process is nearly completely inhibited by 1,10-phenanthroline, a Zn^{2+} chelator that functions as a general metalloprotease inhibitor. On the other hand, a mixture containing serine and cysteine protease inhibitors did not block the removal of the MycHis tag from ADAM19(EC)-MycHis. Taken together, these results indicate that this proteolysis event is mediated by a metalloprotease. Finally, the fact that the catalytic mutant remains intact after identical treatment shows that the removal of the tag in recombinant ADAM19 is autocatalytic. This provides a potential explanation for why, compared with its inactive counterpart, wild type ADAM19(EC)-MycHis always appeared to be present in lower amounts in the conditioned media of infected Hi5 cells.

The autodegradation of ADAM19 appears to be greatly enhanced at pH 8.5, because the loss of the MycHis tag is already observed at 4 °C at this pH (Fig. 2, *lower panels*). Interestingly, ADAM19(EC$_{E/A}$)-MycHis, otherwise very stable, becomes protease-sensitive in the presence of 1,10-phenanthroline. This observation suggests that the removal of the catalytic zinc atom is sufficient to disrupt the stability and structure of ADAM19 rendering it accessible to other proteases present in the supernatant. When analyzed under similar conditions, wild type recombinant ADAM19(MP)-MycHis also undergoes a metalloprotease-mediated proteolysis with a basic optimum pH (data not shown). However, both the mutant and wild type proteins are also sensitive to non-metalloprotease activities present in the conditioned culture supernatant at both pH 7.4 and 8.5 (not shown). Considering the higher degree of stability of ADAM19(EC), we retained this construct for the further evaluation of the catalytic properties of this enzyme.

The recombinant proteins were then purified by metal affinity chromatography (see Fig. 3). The integrity of the recombinant proteases after diverse standard elution conditions was assayed by monitoring their ability to autocatalytically remove the purification tag after incubation at 37 °C. This property was lost after treatment with 0.5 M imidazole or with 3.5 M $MgCl_2$ but was retained when the protease was eluted using 50 mM sodium acetate, pH 5.0, 300 mM NaCl. The purified wild type and mutant 66-kDa protein bands were submitted to N-terminal sequencing. In both cases, the N-terminal sequences were identical and corresponded to the amino acids

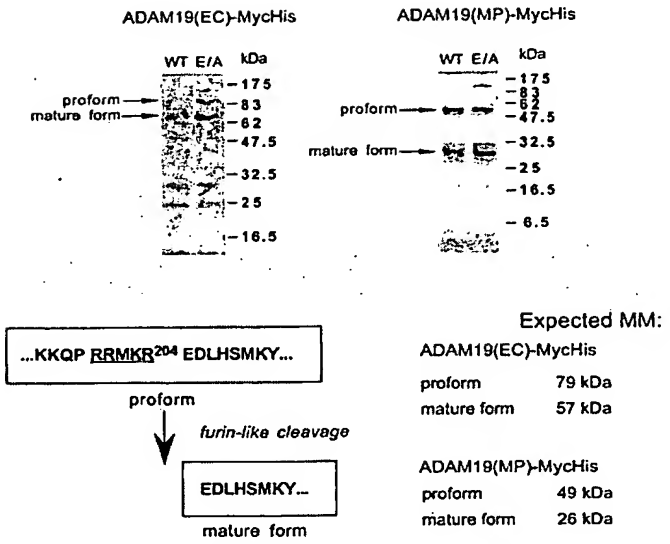

FIG. 3. **SDS-PAGE analysis of purified ADAM19(EC)-MycHis and ADAM19(MP)-MycHis.** *Upper panels* show Gelcode Blue-stained SDS-polyacrylamide gels of purified ADAM19(EC)-MycHis and ADAM19(MP)-MycHis, both wild types (*WT*) and mutants. The *lower panel* shows the ADAM19 protein sequence around the furin-like processing site, at the junction of the prodomain and the metalloprotease domain. Theoretical molecular masses (*MM*) of the recombinant forms of ADAM19 are also indicated.

directly following the furin-like cleavage site present at the junction of the pro- and metalloprotease domains of mouse ADAM19 (RRMKR; Fig. 3, *lower panel* (31)). Consequently, ADAM19(EC)-MycHis appears properly processed in Hi5 cells, presumably by a pro-protein convertase-like activity. Several comigrating bands with lower apparent molecular weights were also present in both wild type and mutant preparations. Attempts to identify these bands by N-terminal microsequencing remained unsuccessful. However, comparison of the proteolytic activity of the wild type recombinant enzyme with that of its inactive counterpart effectively rules out the possible interference of a contaminating protease in the assays used here.

The catalytic properties of ADAM19 were further investigated after purification. Fig. 4*A* confirms that recombinant ADAM19(EC)-MycHis autocatalytically removes its C-terminal tags at basic pH. But ADAM19 was also able to cleave several peptides and proteins, including myelin basic protein (MBP). MBP incubation with wild type ADAM19(EC)-MycHis generates several discrete MBP-related bands with molecular masses ranging from 20 to 3.1 kDa (Fig. 4*B*). This process is blocked by 1,10-phenanthroline, and MBP remains intact when incubated with the catalytically inactive mutant.

MBP product bands generated by the wild type endoprotease were submitted to N-terminal microsequencing. The amino acid sequence of bovine MBP as well as the position of the five ADAM19 cleavage sites are presented in Fig. 4*C*. Bovine MBP can also be cleaved *in vitro* by a broad variety of proteases, including ADAM17/TACE (present work), ADAM28 and ADAM10 (40), and ADAM8 (49). A table comparing the sequences surrounding the cleavage sites by these four ADAMs is shown in Fig. 4*D*. Only one cleavage site appears to be common to all four metalloproteases. A second cleavage site is recognized by ADAM19, ADAM28, and ADAM10 but not by TACE. The alignment of the sequences surrounding these two sites does not reveal any obvious homology.

As shown in Fig. 4*B*, wild type ADAM19(EC)-MycHis self-degradation also leads to the formation of a main product of 37 kDa. N-terminal sequencing of this protein band reveals a

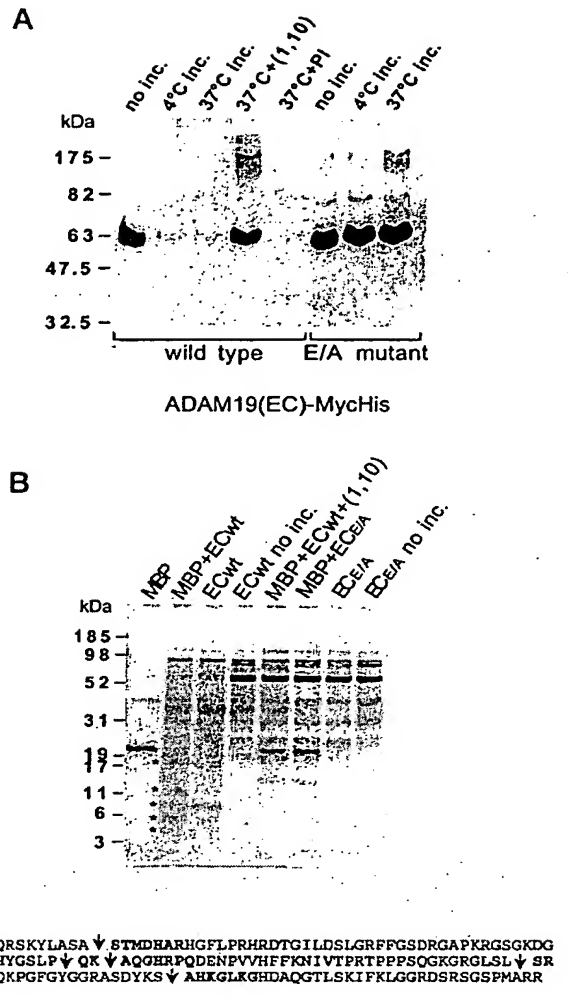

FIG. 4. **ADAM19 proteolytic activity.** *A*, self-proteolysis of purified recombinant ADAM19(EC)-MycHis analyzed by Western blot using the anti-Myc antibody. Lanes labeled *no inc.* (no incubation) correspond to control aliquots kept at −20 °C. Incubations were carried out for 16 h at either 4 or 37 °C. Inhibitor concentrations are as in Fig. 2 (*1,10*) stands for 1,10-phenanthroline, and *PI* indicates protease inhibitor mixture. *B*, MBP degradation assay. MBP was incubated with or without aliquots of wild type (*wt*) or mutated ADAM19(EC)-MycHis for 6 h at 37 °C. 1,10-Phenanthroline at a 1 mM final concentration was included in the *5th lane*. Control lanes showing the band profiles of the enzymes alone after incubation (*ECwt* and $EC_{E/A}$) or without incubation (*ECwt* and $EC_{E/A}$ *no inc.*) are also presented. *Asterisks* indicate MBP degradation products that were N-terminally sequenced. *C*, amino acid sequence of bovine MBP. *Arrows* point at ADAM19(EC)-MycHis cleavage sites. N-terminal sequences of MBP products identified are in *boldface*. *D*, table of MBP cleavage sites used by ADAM19, TACE (ADAM17), ADAM28 (40), and ADAM10 (40). The *upper row* lists cleavage sites common to several or all ADAMs, and the *lower row* lists cleavage sites specific to a particular enzyme.

sequence identical to that of the mature 65-kDa enzyme. This indicates that the main autocatalytic cleavage must occur C-terminal to the metalloprotease domain and thus must leave

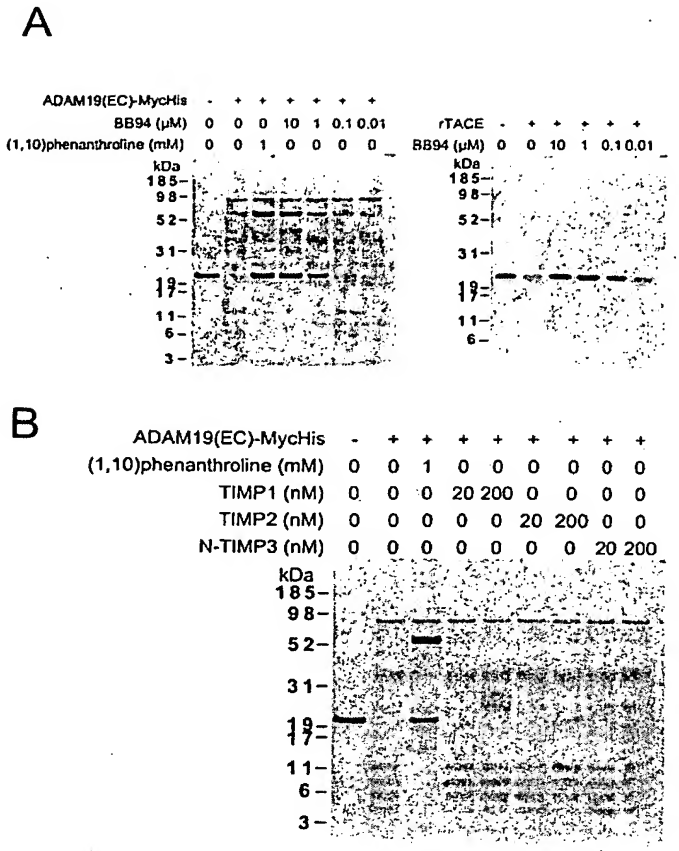

FIG. 5. **ADAM19(EC)-MycHis inhibitor profile.** *A*, MBP was incubated with an aliquot of purified ADAM19(EC)-MycHis (*left panel*) or 50 ng of recombinant TACE (*right panel*) for 1 h at 37 °C in the absence or presence of increasing concentrations of the hydroxamic inhibitor BB94 (batimastat). *B*, effect of TIMP-1, TIMP-2, and His-tagged N-TIMP-3 on MBP degradation by ADAM19(EC)-MycHis.

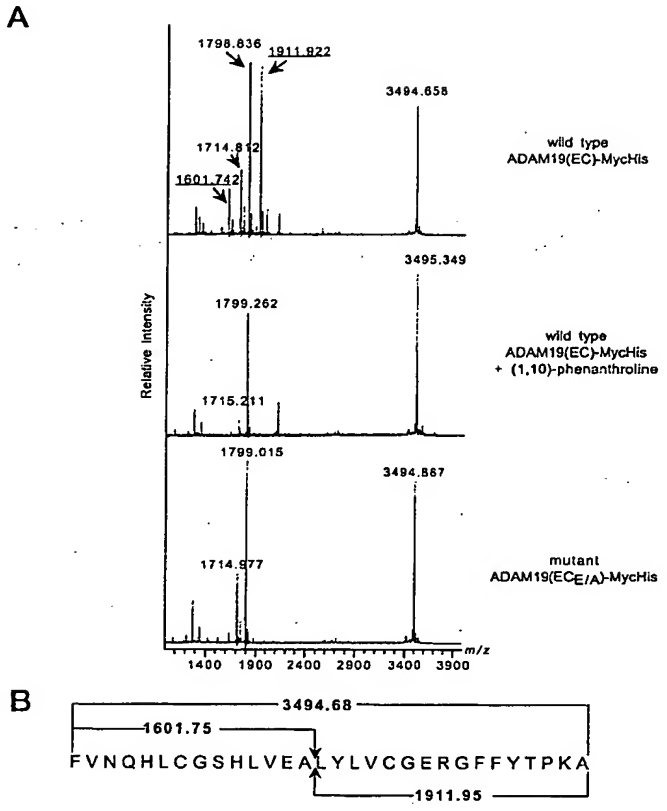

C

ADAM19	TACE	ADAM9	MMP-1
SHLVEA↓LYLVCG	LVEALY↓LVCGER	LVEALY↓LVCGER ERGFFY↓TPKA	LVEALY↓LVCGER

FIG. 6. **ADAM19 activity toward insulin B chain.** *A*, MALDI-reTOF analysis of insulin B chain fragments produced by ADAM19. 100 μM oxidized insulin B chain was incubated for 6 h with an aliquot of purified wild type ADAM19(EC)-MycHis in the presence or absence of 1 mM 1,10-phenanthroline or with an aliquot of inactive mutant. Mass spectrometric traces of resulting products are presented. Peaks at 1799 and 1715 are nonspecific. *B*, insulin B chain cleavage site by ADAM19. *C*, insulin B chain cleavage sites by several ADAM proteins. TACE, ADAM9, and MMP-1 data are from Ref. 41.

this domain intact. Whether this N-terminal fragment of the protease is still active remains to be determined. However, the fact that the C-terminal 28-kDa complementary product cannot be detected by Western blot (data not shown) suggests that multiple internal cleavages occur in the C-terminal portion of ADAM19, *i.e.* within the disintegrin domain and cysteine-rich region. We also note that a band of about 76 kDa, presumably related to the pro-form, is decreased in intensity following incubation at 37 °C in both wild type and mutant ADAM19 and that this decrease is not inhibited by 1,10-phenanthroline. However, because MBP is not cleaved by the catalytically inactive ADAM19(EC$_{E/A}$) mutant, and because cleavage of MBP by wild type ADAM19 is completely blocked by 1,10-phenanthroline, this minor contaminant activity does not affect the interpretation of our results.

To characterize further the catalytic activity of ADAM19, we studied its sensitivity to various metalloprotease inhibitors. Similarly to other ADAMs characterized to date, ADAM19 is inhibited by the hydroxamic acid-based competitive metalloprotease inhibitor BB94, also known as batimastat (Fig. 5*A*, *left panel*). However, although inhibition of MBP cleavage by TACE through BB94 is clearly detectable at 10 nM (Fig. 5*A*, *right panel*, TACE k_i for BB94 is 11 nM (17)), recombinant ADAM19 requires higher concentrations of BB94 for inhibition (Fig. 5*A*, *left panel*).

TIMPs are increasingly used in cell-based systems to characterize metalloproteases implicated in shedding events (14, 53–56). Therefore, their action on MBP cleavage by recombinant ADAM19 was also assayed. No effect of up to 200 nM TIMP1, TIMP2, or N-TIMP3 was observed (Fig. 5*B*). At these concentrations, TIMPS are known to strongly inhibit matrix metalloproteases (49, 57).

We also investigated the cleavage selectivity of ADAM19 by using the oxidized insulin B chain (Fig. 6, *A–C*), a peptide known to be cleaved by several other ADAMs, and various dinitrophenyl-labeled peptides corresponding to the 12 amino acids surrounding the membrane-proximal processing site of selected shed proteins (KL-1, TRANCE, TNFα, p55, and p75 TNFα receptors (TNF-R75 and TNF-R55) and interleukin-6 receptor, see Table I). As shown in Fig. 6, *A* and *B*, ADAM19 cleaves the insulin B chain at a single site (Ala^{14}–Leu^{15}). Interestingly, this site differs from that utilized by TACE, ADAM9, and MMP1 (Tyr^{16}–Leu^{17}; Fig. 6*C* (41)). Among the 6 peptides that mimic the cleavage site of shed proteins assayed here, only three were cleaved by ADAM19 (Table I). KL-1 peptide was cleaved at the physiological cleavage site (58), and TRANCE was processed at one of the cleavage sites used in

TABLE I
ADAM19 proteolytic activity toward synthetic peptides reproducing the membrane-proximal cleavage site of proteins known to be shed by metalloproteases

Peptides at the final concentration of 100 μM were incubated in 50 mM Tris-HCl pH 8.5, 150 mM NaCl for 6 h at 37 °C with an aliquot of wild type purified enzyme in the presence or absence of 1 mM 1,10-phenanthroline or with an aliquot of inactive mutant. Products were identified by MALDI-reTOF mass spectrometry. NC, not cleared. IL-6R, interleukin-6 receptor.

	Predicted cleavage site	ADAM19
KL-1	LPPVAA ↓ SSLRND	LPPVAA ↓ SSLRND
TRANCE	IVGPQR ↓ F ↓ SGAPA	IVGPQR ↓ FSGAPA
TNFα	SPLAQA ↓ VRSSSR	SPLAQAVR ↓ S ↓ SSR
TNF-R75	SMAPGA ↓ VHLPQP	NC
TNF-R55	LPQIEN ↓ VKGTED	NC
IL-6R	TSLPVQ ↓ DSSSVP	NC

COS-7 and CHO cells (14). However, ADAM19 cleaved the TNF-α peptide (59) at two different sites. Again, no consensus or sequence homology between the cleavage sites could be identified.

The ability of ADAM19 to cleave TNFα, TRANCE, and KL-1 peptides *in vitro* prompted us to evaluate the potential role of ADAM19 in shedding the corresponding full-length substrate proteins in cell-based assays. To increase the sensitivity of detection of the precursor and shed forms of the molecules studied, we used expression plasmids encoding full-length TNFα, TRANCE, and KL-1 fused to an AP module. The plasmids were engineered in a way that the AP module was present in the extracellular domain of the membrane proteins and was released into the culture medium after shedding. A schematic representation of the three fusion proteins is presented in Fig. 7*A*.

TNFα is considered to be a *bona fide* ADAM17/TACE substrate (17, 18). To assess the potential involvement of ADAM19 in TNFα shedding, we expressed TNFα-AP in primary mEFs isolated from either wild type embryos or embryos deficient for ADAM19. The amount of TNFα constitutively released over 1 h, or shed within 1 h after stimulation by either 25 ng/ml PMA or 100 μM PV, was assayed by 8% SDS-PAGE, and the AP activity was visualized in the gel using NBT/BCIP. Fig. 7*B* shows that both wild type and ADAM19-deficient mEFs were able to shed TNFα in a constitutive manner. Additionally, no difference between the amounts of shed TNFα after stimulation by either PMA or PV could be observed between *adam19−/−* and wild type mEFs. Thus, ADAM19 is not required for constitutive, PMA-, or PV-induced TNFα shedding in primary fibroblasts.

The effect of ADAM19 on TRANCE shedding from the plasma membrane was first assayed in COS-7 cells (Fig. 7*C*). COS-7 cells cotransfected with TRANCE-AP expression plasmid and pcDNA3 only released very low amounts of soluble TRANCE. Similarly, low levels of constitutive shedding were observed in cells expressing TACE or an inactive full-length ADAM19 ($ADAM19_{E/A}$). However, coexpression of wild type ADAM19 greatly increased the amount of TRANCE released into the supernatant, suggesting that ADAM19 is able to cleave membrane-anchored TRANCE in transfected COS-7 cells. On the other hand, no obvious difference could be observed in the levels of TRANCE shed by wild type and ADAM19-deficient mEFs (data not shown). The levels of constitutive and PMA-stimulated shedding were very low in both cell types, and no difference in the PV stimulated shedding of TRANCE was observed in the absence of ADAM19, consistent with results reported previously (14).

Finally, we investigated the importance of ADAM19 in KL-1 shedding (Fig. 7*D*). COS-7 cells transfected with the AP-KL-1 expression vector together with $pcDNA_3$ or the mutant $ADAM19_{E/A}$ expression plasmid both released increased amounts of KL-1 after stimulation by either PMA or PV (Fig. 7*D, upper panel*). Interestingly, the expression of full-length wild type ADAM19 in COS-7 cells strongly reduced the stimulated release of KL-1. A Western blot analysis shows that both the wild type protease and the mutant were expressed (Fig. 7*D, lower left panel*). The fact that the inactive mutant of ADAM19 has very little, if any, effect on stimulated shedding of AP-KL-1 demonstrates that the catalytic activity of ADAM19 is responsible for the reduction in KL-1 shedding. Spectrometric quantification of soluble AP-KL-1 present in the conditioned medium of transfected COS-7 cells revealed that the shedding response to PMA or PV in the presence of wild type ADAM19 is only 15–26% that of the control transfection ($pCDNA_3$). Consistent with these observations, ADAM19-deficient mEFs show an increased response to PMA and PV compared with wild type mEFs (Fig. 7*D, lower right panel*). Quantitative data from three independent experiments show a 1.2–1.7-fold higher PMA response in *adam19−/−* cells compared with control cells and a 1.5–1.8-fold higher PV response.

DISCUSSION

Here we present the first biochemical characterization of mouse ADAM19, a metalloprotease-disintegrin protein with an essential role in cardiovascular morphogenesis.[2] The first evidence for catalytic activity of the recombinant protein composed of the soluble ectodomain of ADAM19 was provided by the autocatalytic proteolysis within its disintegrin or cysteine-rich domain. This processing was unexpected, because full-length ADAMs usually do not undergo autocatalytic processing in these domains in intact cells. However, autoproteolysis of ADAM12 (60) and ADAM13 (61) has been observed after cells are lysed in non-ionic detergents in the absence of a metalloprotease inhibitor such as 1,10-phenanthroline. This suggests that anchorage of an ADAM to the plasma membrane somehow prevents autodegradation, and might thus be important for the stability of these metalloproteases in cells. It remains to be determined whether this interaction with the plasma membrane also has a role in regulating the catalytic activity of ADAM19 toward other substrates in cells in addition to preventing autocatalysis.

This study reports the first identification of peptide substrates that are turned over by ADAM19 *in vitro*, as well as of their cleavage sites. Among those peptides, several are also cleaved by other members of the ADAM family. Myelin basic protein, for example, is cut *in vitro* by ADAM8 (49), ADAM10 (40), TACE, and ADAM28 (40), and the oxidized insulin B chain is proteolyzed by TACE and ADAM9, as well as by MMP-1 (41). Interestingly, although some peptide bonds are recognized by more than one enzyme, the comparison of the amino acid sequences surrounding the cleavage sites fails to highlight any particular consensus or homology neither for ADAM19 substrates nor for those of other ADAMs. Together with the fact that most of the cleavage sites of shed proteins are localized in the membrane-proximal region, this suggests that secondary structure of the substrate may play an important role in the recognition by these enzymes. However, as different ADAMs often cleave at adjacent sites in the same peptide, it is likely that these proteases nevertheless have distinct cleavage selectivity.

The ability to monitor the catalytic activity of ADAM19 *in vitro* allowed us to demonstrate that, like all ADAMs characterized to date, ADAM19 is sensitive to both 1,10-phenanthroline and the hydroxamate-based competitive inhibitor, batimastat (BB94). However, when assayed in parallel with the same substrate (MBP), ADAM19 was less sensitive to BB94

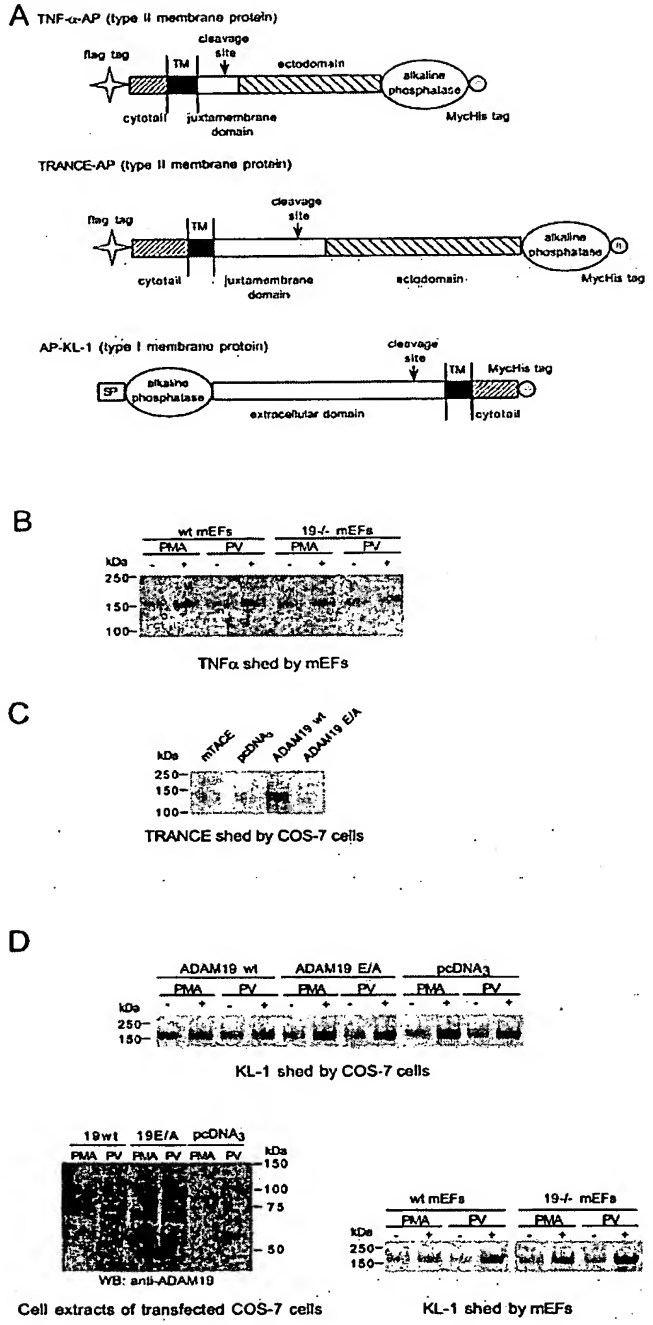

FIG. 7. **Effect of ADAM19 on TNFα, TRANCE, and KL-1 shedding in transfected COS-7 cells and mEFs isolated from wild type and *adam19−/−* mice.** *A*, schematic representation of the AP fusion proteins used in this study. *B*, TNFα-AP shedding. Primary mEFs isolated from wild type or *adam19−/−* embryos were transfected with a TNFα-AP expression vector (45). Soluble TNFα-AP accumulated in the medium during 1 h in unstimulated cells or in cells treated with either PMA or PV was analyzed by 8% SDS-PAGE. The AP activity was visualized by incubating the gel in NBT/BCIP as described (45). *C*, TRANCE-AP shedding. COS-7 cells were transfected with TRANCE-AP expression plasmid together with $pcDNA_3$, $pcDNA_{3.1}$-mTACE, $pcDNA_3$-ADAM19, or $pcDNA_3$-$ADAM19_{E/A}$. Media were collected after 1 h of incubation and analyzed as described in *B*. *D*, AP-KL-1 shedding. Conditioned media from transfected COS-7 cells and wild type or *adam19−/−*mEFs were analyzed as in *B*. Cell lysates from COS-7 cells were examined for expression of wild type or mutant ADAM19 by 8% SDS-PAGE under non-reducing conditions followed by Western blot using the anti-$ADAM19(EC_{E/A})$EK-FC polyclonal antibody.

than TACE (Fig. 5*A*). TIMPs have become widely used to study shedding processes in cell-based systems, and ADAMs show variable sensitivities to these biological inhibitors. For example, TACE activity is blocked by TIMP-3, but not by TIMP-1, -2, or -4 (62), whereas ADAM10 is sensitive to both TIMP-1 and -3 (50). ADAM9 is insensitive to TIMP-1, -2, and -3 (49), ADAM28 to TIMP-1 and -2 (40), and ADAM8 to all four TIMPs (49). ADAM-12, the closest homologue of ADAM19, is sensitive to TIMP-3 but not to TIMP-1 and -2 (63). Thus, ADAM19 belongs to a small group of metalloproteases that are not inhibited by TIMPs 1–3. TIMPs are therefore likely to be valuable tools to assist in narrowing down the list of candidate sheddases for any given substrate.

This study also shows that ADAM19 is most active at basic pH. This basic pH optimum is similar to that of several other metalloproteases, including ADAM12 (63), as well as members of more distant metalloprotease families such as *N*-arginine dibasic convertase (64) or meprin A (65, 66). When overexpressed in COS-1 cells, ADAM19 colocalizes with furin, which is likely responsible for its activation (67) in the trans-Golgi network (TGN). Enzymes that function mainly in this cell compartment, such as furin, are known to have a slightly acidic optimum pH (~pH 6) (68), which is close to that of the TGN (pH 6.2) (69). Even though it remains to be determined where, in the cell, ADAM19 actually acts, one possibility is that it cycles between the TGN and the plasma membrane. In this case, the basic pH optimum of ADAM19 may provide a mechanism to keep the mature enzyme inactive until it reaches the cell surface.

In order to determine whether the cleavage site preferences of ADAM19 *in vitro* could help identify candidate substrates of ADAM19 *in vivo*, we incubated ADAM19 with peptides corresponding to the cleavage sites of several proteins that undergo ectodomain shedding (Table I). This approach uncovered three potential ADAM19 substrates, TNFα, TRANCE, and KL-1. The TNFα peptide, which both TACE and ADAM10 cleave at the physiological site Ala^6–Val^7 (17, 18, 51), is cut twice by ADAM19, inbetween Arg^8–Ser^9 and Ser^9–Ser^{10}. The TNFα convertase (TACE/ADAM17) is already clearly established as the major physiologically relevant stimulated sheddase of TNFα (17, 18). The fact that ADAM19(EC)-MycHis cleavage of TNFα peptide did not generate the physiological N terminus of soluble TNF argues against an important role of ADAM19 in the shedding of this growth factor. This was confirmed by investigating the release of the TNFα ectodomain fused to a reporter enzyme (AP) by mEFs derived from wild type and ADAM19-deficient mouse embryos. As presented in Fig. 7*B*, no difference could be observed between the two cell types. Nevertheless, this finding does not exclude the possibility that ADAM19 could contribute to TNFα release in situations where ADAM19 is overexpressed or misregulated.

TRANCE is a TNF family member involved in osteoclastogenesis and dendritic cell survival (70–75). A peptide corresponding to the TRANCE membrane-proximal region is processed by recombinant ADAM19 *in vitro* at a constitutive cleavage site that is used in both COS-7 and CHO cells *in vivo* (14). This site is also cleaved by ADAM17/TACE *in vitro* (76). However, when full-length wild type ADAM17 or ADAM19 was cotransfected with TRANCE in COS-7 cells, we observed a considerable increase in constitutive shedding of TRANCE in the presence of ADAM19 but not ADAM17. Furthermore, no increase in TRANCE shedding was seen when proteolytically inactive ADAM19 ($ADAM19_{E/A}$) was coexpressed. This demonstrates that the catalytic activity of ADAM19 is necessary for increased TRANCE shedding in COS-7 cells. Although ADAM19 is not required for constitutive or activated TRANCE

shedding in mEF cells (14), these results still suggest that ADAM19 could function as a constitutive TRANCE sheddase in cells where it is highly expressed, such as in osteoblasts (31). Further studies will be necessary to address this possibility.

Finally, KL-1, a ligand for the kit receptor tyrosine kinase, also emerged as a candidate ADAM19 substrate because the KL-1 peptide was cleaved by ADAM19 *in vitro* at the site that is presumably used *in vivo* (58). KL-1 and KL-2 derive from splice variants of a common mRNA, and both are expressed in a tissue-specific manner (77). KL-1 is efficiently processed and released as a soluble growth factor, whereas KL-2 is less efficiently cleaved and is therefore mainly found as a transmembrane protein. Recently, MMP-9 has been shown to play a significant role in the release of soluble KL (78). However, the fact that soluble KL was still produced in MMP-9-deficient mice, although at lower levels compared with control animals, implies that one or several other proteases are able to process KL. Unexpectedly, we found that overexpression of wild type ADAM19 in COS-7 cells strongly reduced stimulated shedding of KL-1, whereas overexpression of the catalytically inactive mutant did not. Furthermore, we observed enhanced shedding of KL-1 in *adam19−/−* mEFs compared with wild type controls. This suggests that ADAM19 serves as a negative regulator of KL-1 shedding. Different possible mechanisms include an inactivation of the KL-1 sheddase by ADAM19 or activation of an inhibitor of KL-1 shedding. Further studies will be necessary to distinguish between these and other possibilities.

In summary, we report here the first biochemical characterization of mouse ADAM19. We have identified several *in vitro* substrates of the metalloprotease and determined its sensitivity toward inhibitors commonly used to study protein ectodomain shedding. Furthermore, we have shown that ADAM19 affects TRANCE and KL-1 shedding in cell-based systems, raising the possibility that ADAM19 has a role in regulating the function of these molecules *in vivo*. Taken together, the evaluation of the cleavage specificity and inhibitor profile of ADAM19 provides the basis for further studies of its physiological functions.

Acknowledgments—We are grateful to Dr. Gillian Murphy for the generous gift of recombinant TIMP-1 and TIMP-2, to Dr. Hideaki Nagase for recombinant N-TIMP-3, and to Dr. Peter Besmer for KL-1 cDNA. We also thank Lynne Lacomis for N-terminal sequence determination and Claudio Alarcon for help in the production of some of the baculoviruses.

REFERENCES

1. Black, R. A., and White, J. M. (1998) *Curr. Opin. Cell Biol.* **10**, 654–659
2. Schlöndorff, J., and Blobel, C. P. (1999) *J. Cell Sci.* **112**, 3603–3617
3. Primakoff, P., and Myles, D. G. (2000) *Trends Genet.* **16**, 83–87
4. Primakoff, P., Hyatt, H., and Tredick-Kline, J. (1987) *J. Cell Biol.* **104**, 141–149
5. Blobel, C. P., Myles, D. G., Primakoff, P., and White, J. W. (1990) *J. Cell Biol.* **111**, 69–78
6. Blobel, C. P., Wolfsberg, T. G., Turck, C. W., Myles, D. G., Primakoff, P., and White, J. M. (1992) *Nature* **356**, 248–252
7. Jongeneel, C. V., Bouvier, J., and Bairoch, A. (1989) *FEBS Lett.* **242**, 211–214
8. Bode, W., Gomis-Ruth, F. X., and Stockler, W. (1993) *FEBS Lett.* **331**, 134–140
9. Blundell, T. L. (1994) *Struct. Biol.* **1**, 73–75
10. Stocker, W., Grams, F., Baumann, U., Reinemer, P., Gomis-Ruth, F. X., McKay, D. B., and Bode, W. (1995) *Protein Sci.* **4**, 823–840
11. Massague, J., and Pandiella, A. (1993) *Annu. Rev. Biochem.* **62**, 515–541
12. Hooper, N. M., Karran, E. H., and Turner, A. J. (1997) *Biochem. J.* **321**, 265–279
13. Arribas, J., Coodly, L., Vollmer, P., Kishimoto, T. K., Rose-John, S., and Massague, J. (1996) *J. Biol. Chem.* **271**, 11376–11382
14. Schlöndorff, J., Lum, L., and Blobel, C. (2001) *J. Biol. Chem.* **276**, 14665–14674
15. Powell, W. C., Fingleton, B., Wilson, C. L., Boothby, M., and Matrisian, L. M. (1999) *Curr. Biol.* **9**, 1441–1447
16. Haro, H., Crawford, H. C., Fingleton, B., Shinomiya, K., Spengler, D. M., and Matrisian, L. M. (2000) *J. Clin. Invest.* **105**, 143–150
17. Moss, M. L., Jin, S.-L. C., Milla, M. E., Burkhart, W., Cartner, H. L., Chen, W.-J., Clay, W. C., Didsbury, J. R., Hassler, D., Hoffman, C. R., Kost, T. A., Lambert, M. H., Lessnitzer, M. A., McCauley, P., McGeehan, G., Mitchell, J., Moyer, M., Pahel, G., Rocque, W., Overton, L. K., Schoenen, F., Seaton, T., Su, J.-L., Warner, J., Willard, D., and Becherer, J. D. (1997) *Nature* **385**, 733–736
18. Black, R., Rauch, C. T., Kozlosky, C. J., Peschon, J. J., Slack, J. L., Wolfson, M. F., Castner, B. J., Stocking, K. L., Reddy, P., Srinivasan, S., Nelson, N., Boiani, N., Schooley, K. A., Gerhart, M., Davis, R., Fitzner, J. N., Johnson, R. S., Paxton, R. J., March, C. J., and Cerretti, D. P. (1997) *Nature* **385**, 729–733
19. Peschon, J. J., Slack, J. L., Reddy, P., Stocking, K. L., Sunnarborg, S. W., Lee, D. C., Russel, W. E., Castner, B. J., Johnson, R. S., Fitzner, J. N., Boyce, R. W., Nelson, N., Kozlosky, C. J., Wolfson, M. F., Rauch, C. T., Cerretti, D. P., Paxton, R. J., March, C. J., and Black, R. A. (1998) *Science* **282**, 1281–1284
20. Reddy, P., Slack, J. L., Davis, R., Cerretti, D. P., Kozlosky, C. J., Blanton, R. A., Shows, D., Peschon, J. J., and Black, R. A. (2000) *J. Biol. Chem.* **275**, 14608–14614
21. Rio, C., Buxbaum, J. D., Peschon, J. J., and Corfas, G. (2000) *J. Biol. Chem.* **275**, 10379–10387
22. Pan, D., and Rubin, J. (1997) *Cell* **90**, 271–280
23. Sotillos, S., Roch, F., and Campuzano, S. (1997) *Development* **124**, 4769–4779
24. Lieber, T., Kidd, S., and Young, M. W. (2002) *Genes Dev.* **16**, 209–221
25. Buxbaum, J. D., Liu, K. N., Luo, Y., Slack, J. L., Stocking, K. L., Peschon, J. J., Johnson, R. S., Castner, B. J., Cerretti, D. P., and Black, R. A. (1998) *J. Biol. Chem.* **273**, 27765–27767
26. Slack, B. E., Ma, L. K., and Seah, C. C. (2001) *Biochem. J.* **357**, 787–794
27. Lammich, S., Kojro, E., Postina, R., Gilbert, S., Pfeiffer, R., Jasionowski, M., Haass, C., and Fahrenholz, F. (1999) *Proc. Natl. Acad. Sci. U. S. A.* **96**, 3922–3927
28. Koike, H., Tomioka, S., Sorimachi, H., Saido, T. C., Maruyama, K., Okuyama, A., Fujisawa-Sehara, A., Ohno, S., Suzuki, K., and Ishiura, S. (1999) *Biochem. J.* **343**, 371–375
29. Weskamp, G., Cai, H., Brodie, T., Higashyama, S., Manova, K., Ludwig, T., and Blobel, C. (2002) *Mol. Cell. Biol.* **22**, 1537–1544
30. Yagami-Hiromasa, T., Sato, T., Kurisaki, T., Kamijo, K., Nabeshima, Y., and Fujisawa-Sehara, A. (1995) *Nature* **377**, 652–656
31. Inoue, D., Reid, M., Lum, L., Krätzschmar, J., Weskamp, G., Myung, Y. M., Baron, R., and Blobel, C. P. (1998) *J. Biol. Chem.* **273**, 4180–4187
32. Alfandari, D., Wolfsberg, T. G., White, J. M., and DeSimone, D. W. (1997) *Dev. Biol.* **182**, 314–330
33. Van Eerdewegh, P., Little, R. D., Dupuis, J., Del Mastro, R. G., Falls, K., Simon, J., Torrey, D., Pandit, S., McKenny, J., Braunschweiger, K., Walsh, A., Liu, Z., Hayward, B., Folz, C., Manning, S. P., Bawa, A., Saracino, L., Thackston, M., Benchekroun, Y., Capparell, N., Wang, M., Adair, R., Feng, Y., Dubois, J., FitzGerald, M. G., Huang, H., Gibson, R., Allen, K. M., Pedan, A., Danzig, M. R., Umland, S. P., Egan, R. W., Cuss, F. M., Rorke, S., Clough, J. B., Holloway, J. W., Holgate, S. T., and Keith, T. P. (2002) *Nature* **418**, 426–430
34. Yoshinaka, T., Nishii, K., Yamada, K., Sawada, H., Nishiwaki, E., Smith, K., Yoshino, K., Ishiguro, H., and Higashiyama, S. (2002) *Gene (Amst.)* **282**, 227–236
35. Gunn, T. M., Azarani, A., Kim, P. H., Hyman, R. W., Davis, R. W., and Barsh, G. S. (2002) *BMC Genet.* **3**, 2
36. Fritsche, J., Moser, M., Faust, S., Peuker, A., Buttner, R., Andreesen, R., and Kreutz, M. (2000) *Blood* **96**, 732–739
37. Wei, P., Zhao, Y. G., Zhuang, L., Ruben, S., and Sang, Q. X. (2001) *Biochem. Biophys. Res. Commun.* **280**, 744–755
38. Shirakabe, K., Wakatsuki, S., Kurisaki, T., and Fujisawa-Sehara, A. (2001) *J. Biol. Chem.* **276**, 9352–9358
39. Lum, L., Reid, M. S., and Blobel, C. P. (1998) *J. Biol. Chem.* **273**, 26236–26247
40. Howard, L., Zheng, Y., Horrocks, M., Maciewicz, R. A., and Blobel, C. P. (2001) *FEBS Lett.* **498**, 82–86
41. Roghani, M., Becherer, J. D., Moss, M. L., Atherton, R. E., Erdjument-Bromage, H., Arribas, J., Blackburn, R. K., Weskamp, G., Tempst, P., and Blobel, C. P. (1999) *J. Biol. Chem.* **274**, 3531–3540
42. Erdjument-Bromage, H., Lui, H., Lacomis, L., Grewal, A., Annan, R. S., McNulty, D. E., Carr, S. A., and Tempst, P. (1998) *J. Chromatogr. A* **826**, 167–181
43. Wilkins, M. R., Lindskog, I., Gasteiger, E., Bairoch, A., Sanchez, J. C., Hochstrasser, D. F., and Appel, R. D. (1997) *Electrophoresis* **18**, 403–408
44. Tempst, P., Geromanos, S., Elicone, C., and Erdjument-Bromage, H. (1994) *Methods Companion Methods Enzymol.* **6**, 248–261
45. Zheng, Y., Schlondorff, J., and Blobel, C. P. (2002) *J. Biol. Chem.* **277**, 42463–42470
46. Wong, B. R., Rho, J., Arron, J., Robinson, E., Orlinick, J., Chao, M., Kalachikov, S., Cayani, E., Bartlett, F. S., III, Frankel, W. N., Lee, S. Y., and Choi, Y. (1997) *J. Biol. Chem.* **272**, 25190–25194
47. Robertson, E. J. (1987) in *Teratocarcinomas and Embryonic Stem Cells: A Practical Approach* (Robertson, E. J., ed) pp. 71–112, IRL Press at Oxford University Press, Oxford, United Kingdom
48. Milla, M. E., Leesnitzer, M. A., Moss, M. L., Clay, W. C., Carter, H. L., Miller, A. B., Su, J. L., Lambert, M. H., Willard, D. H., Sheeley, D. M., Kost, T. A., Burkhart, W., Moyer, M., Blackburn, R. K., Pahel, G. L., Mitchell, J. L., Hoffman, C. R., and Becherer, J. D. (1999) *J. Biol. Chem.* **274**, 30563–30570
49. Amour, A., Knight, C., English, W., Webster, A., Slocombe, P., Knauper, V., Docherty, A., Becherer, J., Blobel, C., and Murphy, G. (2002) *FEBS Lett.* **524**, 154–158
50. Amour, A., Knight, C. G., Webster, A., Slocombe, P. M., Stephens, P. E., Knauper, V., Docherty, A. J., and Murphy, G. (2000) *FEBS Lett.* **473**, 275–279
51. Rosendahl, M. S., Ko, S. C., Long, D. L., Brewer, M. T., Rosenzweig, B., Hedl, E., Anderson, L., Pyle, S. M., Moreland, J., Meyers, M. A., Kohno, T., Lyons, D., and Lichenstein, H. S. (1997) *J. Biol. Chem.* **272**, 24588–24593
52. Clarke, H. R., Wolfson, M. F., Rauch, C. T., Castner, B. J., Huang, C. P., Gerhart, M. J., Johnson, R. S., Cerretti, D. P., Paxton, R. J., Price, V. L., and Black, R. A. (1998) *Protein Expression Purif.* **13**, 104–110
53. Faveeuw, C., Preece, G., and Ager, A. (2001) *Blood* **98**, 688–695

54. Nath, D., Williamson, N. J., Jarvis, R., and Murphy, G. (2001) *J. Cell Sci.* **114**, 1213–1220
55. Fitzgerald, M. L., Wang, Z., Park, P. W., Murphy, G., and Bernfield, M. (2000) *J. Cell Biol.* **148**, 811–824
56. Kaup, M., Dassler, K., Weise, C., and Fuchs, H. (2002) *J. Biol. Chem.* **277**, 38494–38502
57. Will, H., Atkinson, S. J., Butler, G. S., Smith, B., and Murphy, G. (1996) *J. Biol. Chem.* **271**, 17119–17123
58. Pandiella, A., Bosenberg, M., Huang, E. J., Besmer, P., and Massague, J. (1992) *J. Biol. Chem.* **267**, 24028–24033
59. Pennica, D., Nedwin, G. E., Hayflick, J. S., Seeburg, P. H., Derynck, R., Palladino, M. A., Kohr, W. J., Aggarwal, B. B., and Goeddel, D. V. (1984) *Nature* **312**, 724–729
60. Cao, Y., Kang, Q., Zhao, Z., and Zolkiewska, A. (2002) *J. Biol. Chem.* **277**, 26403–26411
61. Alfandari, D., Cousin, H., Gaultier, A., Smith, K., White, J. M., Darribere, T., and DeSimone, D. W. (2001) *Curr. Biol.* **11**, 918–930
62. Amour, A., Slocombe, P. M., Webster, A., Butler, M., Knight, C. G., Smith, B. J., Stephens, P. E., Shelley, C., Hutton, M., Knauper, V., Docherty, A. J., and Murphy, G. (1998) *FEBS Lett.* **435**, 39–44
63. Loechel, F., Fox, J. W., Murphy, G., Albrechtsen, R., and Wewer, U. M. (2000) *Biochem. Biophys. Res. Commun.* **278**, 511–515
64. Chesneau, V., Pierotti, A. R., Barre, N., Creminon, C., Tougard, C., and Cohen, P. (1994) *J. Biol. Chem.* **269**, 2056–2061
65. Beynon, R. J., Shannon, J. D., and Bond, J. S. (1981) *Biochem. J.* **199**, 591–598
66. Kenny, A. J., and Ingram, J. (1987) *Biochem. J.* **245**, 515–524
67. Kang, T., Zhao, Y. G., Pei, D., Sucic, J. F., and Sang, Q. X. (2002) *J. Biol. Chem.* **277**, 25583–25591
68. Molloy, S. S., Thomas, L., VanSlyke, J. K., Stenberg, P. E., and Thomas, G. (1994) *EMBO J.* **13**, 18–33
69. Miesenbock, G., De Angelis, D. A., and Rothman, J. E. (1998) *Nature* **394**, 192–195
70. Wong, B. R., Josien, R., Lee, S. Y., Sauter, B., Li, H. L., Steinman, R. M., and Choi, Y. (1997) *J. Exp. Med.* **186**, 2075–2080
71. Anderson, D. M., Maraskovsky, E., Billingsley, W. L., Dougall, W. C., Tometsko, M. E., Roux, E. R., Teepe, M. C., DuBose, R. F., Cosman, D., and Galibert, L. (1997) *Nature* **390**, 175–179
72. Lacey, D. L., Timms, E., Tan, H. L., Kelley, M. J., Dunstan, C. R., Burgess, T., Elliott, R., Colombero, A., Elliott, G., Scully, S., Hsu, H., Sullivan, J., Hawkins, N., Davy, E., Capparelli, C., Eli, A., Qian, Y. X., Kaufman, S., Sarosi, I., Shalhoub, V., Senaldi, G., Guo, J., Delaney, J., and Boyle, W. J. (1998) *Cell* **93**, 165–176
73. Yasuda, H., Shima, N., Nakagawa, N., Yamaguchi, K., Kinosaki, M., Mochizuki, S., Tomoyasu, A., Yano, K., Goto, M., Murakami, A., Tsuda, E., Morinaga, T., Higashio, K., Udagawa, N., Takahashi, N., and Suda, T. (1998) *Proc. Natl. Acad. Sci. U. S. A.* **95**, 3597–3602
74. Kong, Y. Y., Yoshida, H., Sarosi, I., Tan, H. L., Timms, E., Capparelli, C., Morony, S., Oliveira-dos-Santos, A. J., Van, G., Itie, A., Khoo, W., Wakeham, A., Dunstan, C. R., Lacey, D. L., Mak, T. W., Boyle, W. J., and Penninger, J. M. (1999) *Nature* **397**, 315–323
75. Theill, L. E., Boyle, W. J., and Penninger, J. M. (2002) *Annu. Rev. Immunol.* **20**, 795–823
76. Lum, L., Wong, B. R., Josien, R., Becherer, J. D., Erdjument-Bromage, H., Schlondorff, J., Tempst, P., Choi, Y., and Blobel, C. P. (1999) *J. Biol. Chem.* **274**, 13613–13618
77. Huang, E. J., Nocka, K. H., Buck, J., and Besmer, P. (1992) *Mol. Biol. Cell* **3**, 349–362
78. Heissig, B., Hattori, K., Dias, S., Friedrich, M., Ferris, B., Hackett, N. R., Crystal, R. G., Besmer, P., Lyden, D., Moore, M. A., Werb, Z., and Rafii, S. (2002) *Cell* **109**, 625–637